Building and Environment 217 (2022) 109091

Contents lists available at ScienceDirect

Building and Environment

journal homepage: www.elsevier.com/locate/buildenv

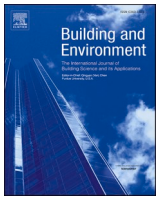

Experimental study on the exposure level of surgical staff to SARS-CoV-2 in operating rooms with mixing ventilation under negative pressure

Yang Bi [a,*], Amar Aganovic [b], Hans Martin Mathisen [a], Guangyu Cao [a]

[a] Norwegian University of Science and Technology, Trondheim, Norway
[b] The Arctic University of Norway, Tromsø, Norway

ARTICLE INFO

Keywords:
Ventilation
Airflow distribution
Negative pressure operating room
Airborne transmission
COVID-19
Surgical microenvironment

ABSTRACT

The purpose of this study was to reveal the exposure level of surgical staff to severe acute respiratory syndrome coronavirus 2 (SARS-CoV-2) from the patient's nose and wound during operations on COVID-19 patients. The tracer gas N_2O is used to simulate SARS-CoV-2 from the patient's nose and wound. In this study, concentration levels of tracer gas were measured in the breathing zones of these surgical staff in the operating room under three pressure difference conditions: −5 pa–15 pa and −25 pa compared to the adjunction room. These influencing factors on exposure level are analyzed in terms of ventilation efficiency and the thermal plume distribution characteristics of the patient. The results show that the assistant surgeon faces 4 to 12 times higher levels of exposure to SARS-CoV-2 than other surgical staff. Increasing the pressure difference between the OR lab and adjunction room can reduce the level of exposure for the main surgeon and assistant surgeon. Turning on the cooling fan of the endoscope imager may result in a higher exposure level for the assistant surgeon. Surgical nurses outside of the surgical microenvironment are exposed to similar contaminant concentration levels in the breathing zone as in the exhaust. However, the ventilation efficiency is not constant near the surgical patient or in the rest of the room and will vary with a change in pressure difference. This may suggest that the air may not be fully mixed in the surgical microenvironment.

1. Introduction

Since the outbreak of the coronavirus disease 2019 (COVID-19) pandemic, health care workers in hospitals have been at high risk of being infected by severe acute respiratory syndrome coronavirus 2 (SARS-CoV-2) [1–4]. The operating room (OR) is a setting where both patients and surgical staff may stay for a long time, which increases the infection risk of surgical staff. The average duration of the majority of operation types is beyond 2 h [5]. Therefore, ORs have also received great attention, and researchers have continuously proposed measures to prevent surgical staff from being infected, including the utilization of personal protective equipment (PPE) [6–8], aerosol boxes [9], and stricter infection control methods [8]. In addition, some hospitals shared their experience in the prevention of infection control in ORs [3,10].

Whether airborne transmission is one of the main modes of transmission for SARS-CoV-2 has been intensively debated since the beginning of the pandemic [11–13]. However, with more research conducted, airborne transmission has been widely recognized as one of the main modes of transmission for SARS-CoV-2. For instance, some studies have found viral ribonucleic acid (RNA) in air samples taken from rooms where COVID-19 patients have stayed [14–16]; other studies have found evidence of aerosol transmission by reviewing past outbreak events [17–20]. Ventilation is then considered to be an effective means of avoiding infection to prevent the spread of airborne transmission virus [21].

Based on the consensus that airborne transmission is one of the main modes of transmission of COVID-19, several measures around the operating room to prevent cross-infection are proposed. Many studies have suggested transforming ventilation in ORs from positive to negative pressure to treat COVID-19 patients [3,22–26]. Compared with positive pressure ventilation, the air outside ORs flows into ORs by penetrating through the cracks of doors and windows of the negative pressure operating room (NPOR), which prevents SARS-CoV-2 from spreading out of the OR.

In contrast, the pressure difference of positive pressure ventilation has no significant effect because there is little air penetrating the room to disturb the airflow distribution in a positive pressure room. At present, there is very little experimental research on the exposure risk of airborne

* Corresponding author.
E-mail address: yang.bi@ntnu.no (Y. Bi).

https://doi.org/10.1016/j.buildenv.2022.109091
Received 17 January 2022; Received in revised form 6 March 2022; Accepted 10 April 2022
Available online 21 April 2022

transmission of COVID-19 in NPOR, except in a few studies using simulation [27,28]. Different countries have different recommendations and requirements regarding the value of the pressure difference of NPORs. For example, the technical specification of surgical cleaning units in China clearly states that patients infected with airborne diseases should be operated on in a negative pressure operating room, but the specification does not indicate a specific pressure value [29]. British ventilation guidelines suggest that the pressure in a negative pressure operating room should be at least - 5 Pa [30]. Both Canadian and CDC guidelines suggest a differential pressure of −2.5 Pa in a negative pressure operating room [31,32].

Equipping PPE has been recommended since the COVID-19 pandemic to prevent surgical staff from being infected in the OR by aerosol viruses released by patients [6,33]. PPE, including respirators, can effectively reduce the wearer's exposure to pollutants. In some cases, nurses, who usually stay far from the patient during operations, should also wear PPE during surgery. However, more than half of OR surgical staff reported a decrease in overall comfort with PPE, and more than 80% of respondents reported increased surgical fatigue. In addition, this combination of PPE can lead to increased respiratory work, reduced vision, reduced touch, and heat stress [34–36]. However, the air change rate in the OR is generally higher than 20 air changes per hour (ACH), and surgical staff away from the operating table may not be exposed to high concentrations of contaminants. This makes it difficult for surgical staff to choose protection equipment that may result in different safety and comfort levels. Therefore, revealing the contaminated exposure level of the breathing zone of surgical staff in the OR is an important indicator to help the medical staff determine whether PPE should be worn.

To date, there have been few studies on the exposure levels of surgical staff to SARS-CoV-2 in ORs. Some of these studies statistically analyze the existing infection cases of surgical staff. In addition to some investigation studies, some experimental and simulation studies were also carried out. Loth Andreas G et al. [37], conducted an experimental study of aerosol exposure levels in patients during tracheotomy and found that 4.8 ± 3.4% of aerosols were removed from surgeons in laminar ORs, compared with ten times as much in nonlaminar ORs. Alex Murr et al. [38]. used optical granulometry to measure aerosol concentrations during endoscopic nasal surgery. Aerosol concentrations at the surgeon's position were significantly increased with the republic bit, a miniature defibrillator. Ban C.H. Sui et al. [39] used a nebulizer to simulate aerosol exposure during intubation and compared aerosol concentrations in the operating room and isolation room, and the results showed that aerosol exposure levels in both rooms were similar. Marc Garbey et al. [40] conducted experimental and simulated studies on the diffusion of surgical smoke in the operating room. The results suggest that opening doors during surgery and inefficient actions by medical personnel can increase indoor pollutant concentrations. However, none of the earlier studies have investigated the effect of different negative pressure conditions on the exposure level of surgical staff to SARS-CoV-2 in ORs with mixing ventilation.

The purpose of this study is to quantify the exposure level of different surgical staff to SARS-CoV-2, which is simulated by tracer gas, under different negative pressure conditions in one OR with mixing ventilation. The findings of this study could be used to assess the infectious risk of surgical staff in ORs and help surgical staff select proper personal protection equipment under the COVID-19 pandemic and other scenarios of airborne transmission diseases.

2. Methodology

2.1. Experimental setup and the OR lab

All measurements for this study were performed in the full-scale OR lab (OR lab) in the Department of Energy and Process Engineering, Norwegian University of Science and Technology (NTNU). The dimensions of the OR Lab are 8.73 m × 7.05 m × 3.25 m (length × width × height), and the volume of the OR lab is 200 m^3. The OR lab has a similar layout and design to an actual OR equipped with a mixing ventilation system in St. Olavs Hospital [41]. Fig. 1 shows the layout of the OR lab and medical equipment.

2.1.1. Ventilation system

The OR lab is equipped with a mixing ventilation system with four supply air diffusers (0.55 m × 0.55 m), as shown in Fig. 1(c), four lower-level exhaust outlets (0.175 m × 0.575 m), and four higher-level exhaust outlets (0.55 m × 0.55 m), as shown in Fig. 1(b). Each lower exhaust grill is connected to a 0.6 m × 0.2 m × 0.315 m plenum box, and each upper exhaust is connected to a 0.315 m × 0.4 m plenum box. The plenum box is equipped with a balancing damper and pressure outlets so that the airflow rate can be measured and controlled. The TSI VelociCalc 9565-P (accuracy of ±1 Pa) was used for pressure measurements in the plenum boxes attached to the exhaust grills and air diffusers to calculate airflow rates. Accordingly, the measuring uncertainty with this method is ±5%. The distribution of exhausted air between the higher and lower exhaust grills for each of the vertical exhaust modules is approximately 1/3 and 2/3, respectively.

2.1.2. OR lab facilities and thermal manikins

The OR lab is equipped with several real medical equipment for ORs, including an anesthesia machine (Fig. 1(a)), an ultrasonic imager (Fig. 1(b)), two endoscope imagers (Fig. 1(d)), two surgical lamps, and an operating table. For some of the other medical devices that do not produce heat, we use manufactured models instead, for instance, two medical ceiling pendants, an instrument table, and some storage cabinets.

Six thermal manikins were used to mimic surgical staff in an OR, including one patient, two surgeons, two nurses, and an anesthesiologist. The specific locations of these manikins can be found in Fig. 1. The surface temperature of the anesthesiologist and the patient can be controlled by the temperature control device. The patient's head, arms, and body were set at 33 °C, 30 °C, and 31 °C, respectively. The head, arms, body, and legs of the anesthesiologist were set at 33 °C, 30 °C, 31 °C and 30 °C, respectively. The heat power of all other manikins is constant power whose value is set according to ASHRAE 55–2020 [42], which can be found in Table 1.

2.2. Experiment set up

A study by Bivolarova et al. [43] found a strong linear relation ($r^2 >$ 0.9) between the mean concentrations of microparticles sized 0.7 and 3.5 μm and the tracer gas nitrous oxide (N_2O) in an indoor ventilated environment. The same study also showed that N_2O, 0.7 μm, and 3.5 μm particles follow almost identical patterns with only a 2%–9% difference in the normalized concentrations. Noakes et al. [44] showed good agreement between the behavior of N_2O tracer gas and 3–5 μm particles in a hospital isolation room. Furthermore, tracer gas has been extensively used in health care-specific studies to assess ventilation system efficiency in removing contaminants [45–47]. In this study, N_2O tracer gas was used to simulate coronaviruses released from the breath and wound of a surgical patient. Studies have shown that aerosolized blood droplets may carry airborne viruses during laparoscopic surgery to release intra-abdominal pressure [48]. Surgical lights will be used at this time, so this study will use two surgical lights throughout all measurements. The sources were released from the nose and wound of the patient separately in each case.

The standards of most countries only set a minimum air change frequency, which is between 18 and 22 ACH [49–52]. The influence of ACH change on air distribution in the operating room has also been studied, so a constant air supply volume of 20 ACHs was used in all these cases. Most standards specify the temperature range, from 18°C to 24 °C [49–52]. In this study, the air temperature was 22 ± 1 °C in the OR lab

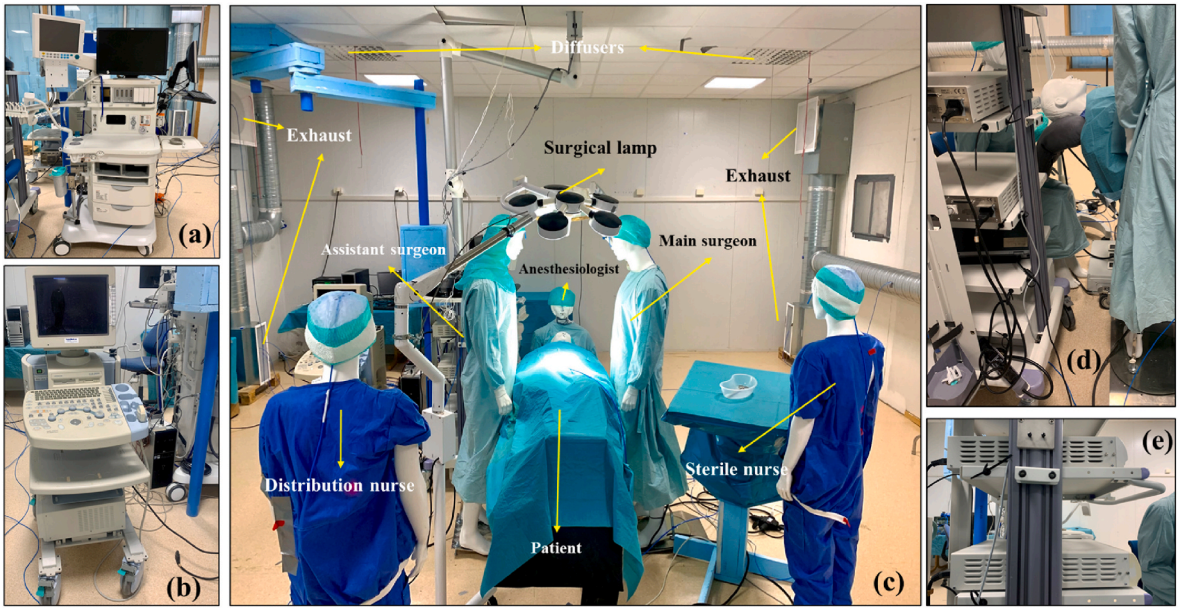

Fig. 1. Medical equipment and layout in the operating room. (a) Anesthesia machine; (b) Ultrasonic imager; (c) the layout of the OR laboratory; (d) Endoscope imager; (e) The cooling fan of the endoscope imager.

Table 1
The heat power of all heat sources in the OR laboratory.

Equipment	Heating power (W)
Surgical lamp 1	61
Surgical lamp 2	74
Supersonic cleaner	45
Endoscope imager	232
Anesthesia machine	136
Main surgeon	150
Assistant surgeon	150
Sterile nurse	140

during measurements. As there is little information on recommended values for negative pressurized ORs, three negative values were used in this study: −5 Pa, −15 Pa, and −25 Pa. The change in pressure difference in the OR lab was achieved by regulating the air extract rate. In total, nine cases were investigated with tracer gas under conditions with or without a ventilation system, different heights of surgical lamps, and different indoor heat intensities. The measurement conditions for each case can be found in Table 2. The air supply volume of all cases is 4000 m^3/h.

2.3. Measurement procedure and instrument

The tracer gas N_2O, which was placed outside of the OR lab, was continually released through a plastic tube (φ33 mm). The flow rate of N_2O is controlled by a gas rotameter connected to the tank. The N_2O flow rate was kept at 0.18 m^3/h (3 L/min) in all cases.

The sampled tracer gas was then sent continuously to a precalibrated Innova 1303 multigas sampler and doser (Brüel & Kjær, Ballerup, Denmark) coupled to an Innova 1302 photoacoustic monitor, which is shown in Fig. 2(a). According to the manufacturer, the repeatability of the Innova 1302 measurements is ±1% under standard conditions. All standard deviations of the measured results performed under conditions without medical equipment were calculated to be under 5% of the mean value. There were six tracer gas measurement points, including exhaust (Point 1), breathing zone of distribution nurse (Point 2), anesthetist (Point 3), sterile nurse (Point 4), main surgeon (Point 5), and assistant surgeon (Point 6).

AirDistSys5000 anemometers were used to measure air temperature and airspeed at 5 × 7 = 35 points in the OR lab, as shown in Fig. 2(b). The lowest measurement points were 10 cm higher than those of the patient. These anemometers measure airspeed and temperature with an accuracy of ±0.02 m/s (accuracy of ±0.2 °C, respectively. The measurement plane is shown in Fig. 2(b). Each measurement lasted for 3 min with a sampling rate of 0.5 Hz and the average values of 90 data were used.

Before each experiment, the OR lab was ventilated for 2 h in advance, the tracer gas was turned on after the indoor temperature was stable and the wall temperature remained unchanged. The sampling time of the Innova 1302 photoacoustic monitor was approximately 60 s/channel, and six channels were measured in sequence, giving 6 min between each measurement at the same location. The total sampling time for one case with two repeated measurements was between 300 and

Table 2
Measurement conditions.

Case	Tracer gas source	Pressure difference	Heat source	Ventilation	Surgical lamp	Air extract rate
1.	Nose	−5 Pa	All on	On	1.95 m	4140 (m^3/h)
2.	Nose	−15 Pa	All on	On	1.95 m	4242 (m^3/h)
3.	Nose	−25 Pa	All on	On	1.95 m	4316 (m^3/h)
4.	Wound	−5 Pa	All on	On	1.95 m	4140 (m^3/h)
5.	Wound	−15 Pa	All on	On	1.95 m	4242 (m^3/h)
6.	Wound	−25 Pa	All on	On	1.95 m	4316 (m^3/h)
7.	Wound	−5 Pa	Endoscope off	On	1.95 m	4140 (m^3/h)
8.	Wound	−5 Pa	All off	On	1.95 m	4140 (m^3/h)
9.	Wound	−5 Pa	All on	On	2.05 m	4140 (m^3/h)

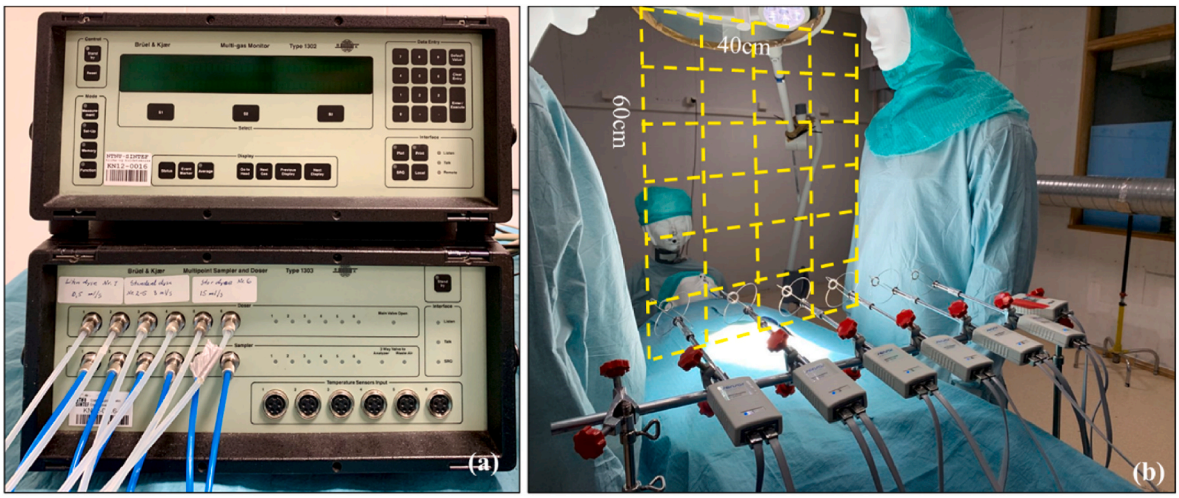

Fig. 2. Experimental equipment and measuring plane. (a) Tracer gas measuring equipment (b) Hot-wire anemometer and the measuring grid.

350 min. The clean-up procedure was performed between two cases to keep the level of N_2O rate below 0.5 ppm, which should be extracted from the measurement value.

2.4. Statistics analysis

Descriptive statistics were used for the analysis of the sampled N_2O levels at six measurement points. Skewness and kurtosis statistics were used to test the assumption of normality for the N_2O levels. Levene's test for equality of variances was used to test the assumption of homogeneity of the variance. Given that the statistical assumptions were met, a 1-way analysis of variance (ANOVA) assessed whether the mean N_2O levels were significantly different between the same measurement points for different cases. If the statistical assumptions were violated, nonparametric Kruskal-Wallis tests were used as an alternative for ANOVA. Kruskal-Wallis tests the stochastic dominance between groups, i.e., whether any randomly measured concentration of N_2O (ppm) from one case is higher or lower than any random concentration from another group. As both ANOVA and Kruskal-Wallis methods do not specify which specific cases were significantly different, significant differences between every two cases for one position were examined using Mann-Whitney U tests in a post hoc fashion. The significance was defined as $p < 0.05$. All analyses were conducted using SPSS version 27. (IBM, Armonk, NY).

2.5. Ventilation effectiveness

Air change efficiency and local air change index category indicators were used to interpret the measured results in this study [53,54]. The air change efficiency, ε, is defined as the ratio between the shortest possible air change time for the air in the room, the nominal time constant, τ_n, and the actual air change time,$\overline{\tau}_e$.

3. Results

3.1. Measurement results of pollutant concentration when tracer gas is released from the nose of a patient (Cases 1–3)

Fig. 3 shows a boxplot of the measured concentration results in Cases 1 to 3 when the tracer gas is released through the patient's nose under three different pressure values. The figure contains information on mean values, medium values, 1.5 interquartile range (IQR), and outliers at different measurement points. Due to the large difference in data at different points, the y axis is displayed as a logarithmic axis. This figure shows that the highest concentration appears at point 6, the breathing zone of the assistant surgeon, which is 333.1 ppm, 284.7 ppm, and 186.0 ppm under three different pressure conditions: −5 Pa, - 15 Pa, and −25 Pa, respectively. This was followed by point 5, at the breathing zone of the main surgeon, whose mean concentration at the breathing zone was 74.3 ppm 48.7 ppm, and 40.0 ppm. The lowest concentration results

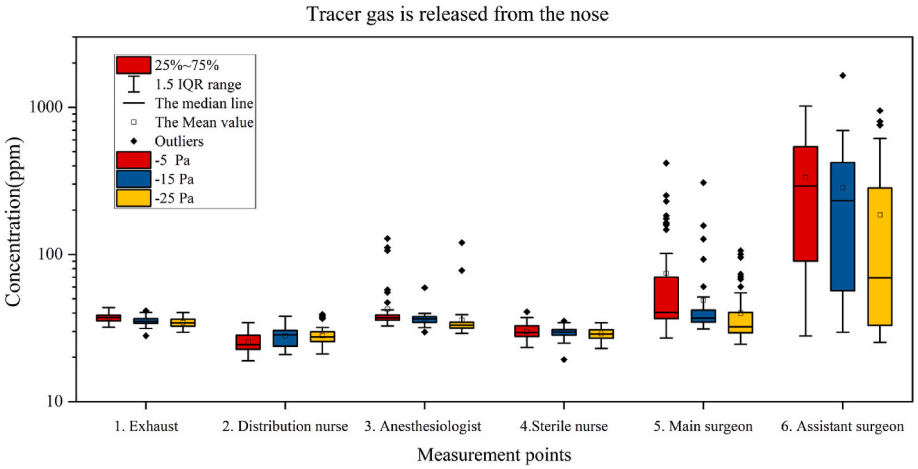

Fig. 3. Boxplot of concentration results when tracer gas is released from patient's nose.

were found at point 2, the breathing zone of the distribution nurse, at 25.5 ppm. 28.0 ppm and 28.1 ppm, which are lower than the exhaust concentration. The concentration at point 3, the breathing zone of the anesthesiologist, was slightly higher than that in the exhaust at between 103% (35.8 ppm) and 114% (42.5 ppm). The concentration results at point 4, the breathing zone of the sterile nurse, showed a value of 29.0 ppm and slightly changed with the change in pressure difference. Considering the effect of pressure change on concentration, except for the distribution nurse, the mean value of concentration at all points decreases with increasing pressure. Despite this, except for two surgeons, the concentrations in the breathing zone of other surgical staff were not significantly different from those of the exhaust. This may indicate that the supply air is fully mixed with room air outside the surgical microenvironment.

3.2. Measurement results of pollutant concentration when tracer gas is released from the surgical wound (Cases 4–6)

Fig. 4 shows the boxplot of concentration results at each point in Case 4-Case 6 as tracer gas is released from the wound of the patient.

The highest mean concentrations were found at point 6, reaching 443.0 ppm, 412.0 ppm, and 446.0 ppm at −5 pa, −15 Pa, and −25 Pa, respectively, all of which were more than 12 times the mean value of the concentration at point 1, the exhaust. This was followed by concentration point 5, whose mean concentration reached 102.0 ppm, 61.0 ppm, and 62.0 ppm at −5 Pa, −15 Pa, and −25 Pa, respectively, which were 293%, 185%, and 190% of the exhaust concentration. The mean concentrations of other measurement points were close to the mean concentration at the exhaust, among which the lowest concentrations were 38.4 ppm, 33.2 ppm, and 28.3 ppm at −5 Pa, −15 Pa, and −25 Pa, respectively, at point 4. Considering the influence of the pressure difference on the concentration, we found that with increasing pressure difference, the concentration of all the measuring points decreased except the concentration at point 2, which shows a similar trend as Case 1 to Case 3. The difference comparing the first three cases is that the concentration at point 6 does not change drastically with the change in the pressure difference.

3.3. Measurement results of reference experimental settings (Cases 7–9)

Cases 7–9 changed some experimental settings based on Case 4 and compared the differences in different influencing factors. In Case 7, the endoscopic equipment was turned off, and all heat sources in Case 8 were turned off, while in Case 9, the operating lamp was moved up 10 cm. The results of the 4 cases of Case 4 and Case 7–9 are shown in Fig. 5. After the endoscope was turned off (Case 7), the concentration result of Point 5 (185.5 ppm) showed little difference from point 6 (199.1 ppm). However, when the endoscope was turned on, the concentration at point 6 (443.3 ppm) was much higher than that at point 5 (102.4 ppm) because points 1, 2, and 4 are similar in these two cases, both in terms of the mean and the degree of dispersion of the data. The average at Point 3 shows a decrease from 41.1 ppm to 35.6 ppm.

When we turned off all the heat sources (Case 8) in the room, including all manikins, the concentrations at points 5 and 6 dropped dramatically, while the concentration at points 2 and 3 increased. This suggests that in the absence of a thermal plume, pollutants may spread horizontally rather than vertically. In Case 9, the surgical lamp was raised by 10 cm, and the results showed that the concentration at point 2 and point 4 decreased compared with those in Case 4, while the concentration at point 6 increased. Original data for of all measurements can be found in Appendix 1 and Appendix 2.

3.4. Air change efficiency and local air change index

The air change efficiency and local air change index were used to evaluate the performance of airflow distribution at these measurement points. Air change efficiency represents the performance of the air distribution of the ventilation system in the room. The calculated value of the air change efficiency of the OR is 49.24%, 49.91%, and 50.18% at −5 Pa, −15 Pa, and −25 Pa, respectively. For a mixing ventilated room, the ideal air change efficiency is 50%, and it may be lower due to air recirculation and higher due to a better air distribution method.

Fig. 6 shows the local air change index by using the measurement results. As explained in Section 2.5, the local air change index indicates the ratio of the time it takes for air to reach the exhaust to the time it takes to reach a specific position in the room. The ideal value in a mixing ventilation room is 100%. If the index at a point is less than 100%, it means that the air reaches this point more slowly than the air reaches the exhaust, and vice versa. Fig. 6 shows the local air change index from point 2 to point 6. From the figure, we can see that the local air change index of points 2, 3, and 4 is similar to the trend of pressure; that is, the increase in pressure will increase the local air change index of these points. Among them, point 3 has the largest variation range, which increases from 75.26%, which is the lowest value, at −5 Pa to 108.56% at −25 Pa. However, this value is the lowest among the three points at −5 Pa and −15 Pa. Among the three points, the index of point 4 is the highest in each pressure difference condition, which are 104.47%, 111.94%, and 119.94% at −5 Pa, −15 Pa, and −25 Pa, respectively. The index value of point 2 also increased steadily from 92.38% at −5 Pa to 105.45% at −25 Pa.

The local air change index at point 5 and point 6 is greater than 100% under all pressure conditions, but it does not show the same change

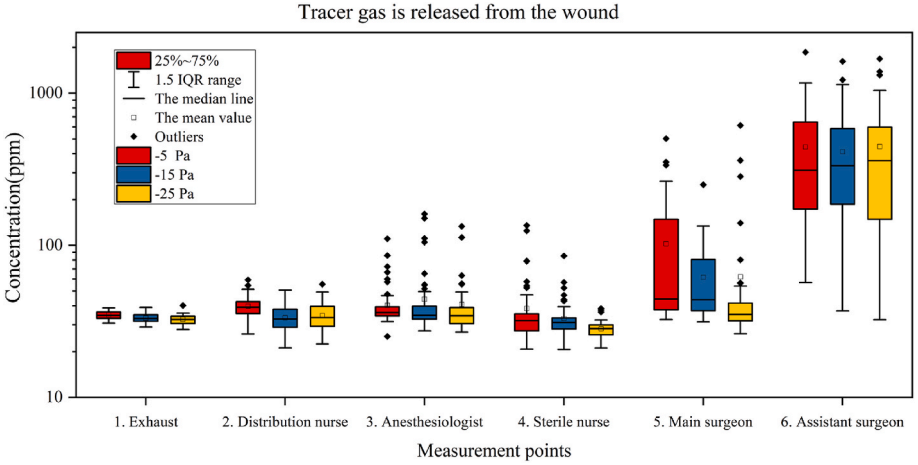

Fig. 4. Boxplot of concentration results when tracer gas is released from patient's wound.

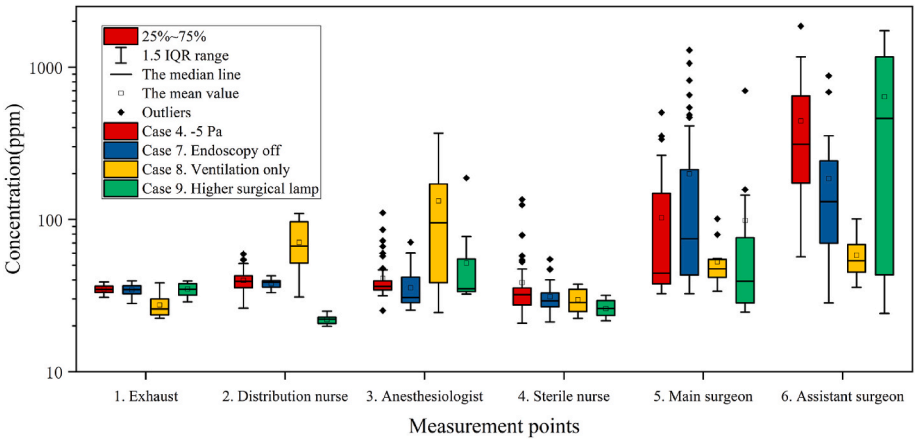

Fig. 5. Comparison of the concentration distribution of closed endoscopy in Case 4.

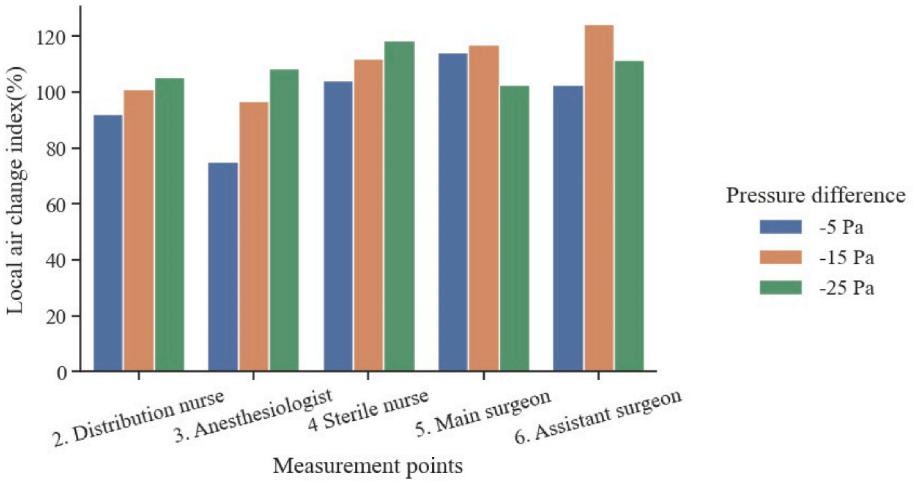

Fig. 6. Local air change index of each surgical staff breathing zone.

pattern as the first three points. As the pressure increased, the local air change index at point 5 increased slightly from 114.28% (-5 Pa) to 117.11% (-15 Pa) but decreased to 102.69% (-25 Pa). The local air change index at point 6 also experienced an increase, from 102.59% (-5 Pa) to 124.49 (-15 Pa), and then decreased to 111.73% at −25 Pa.

The original measured data and the calculated value of λ can be

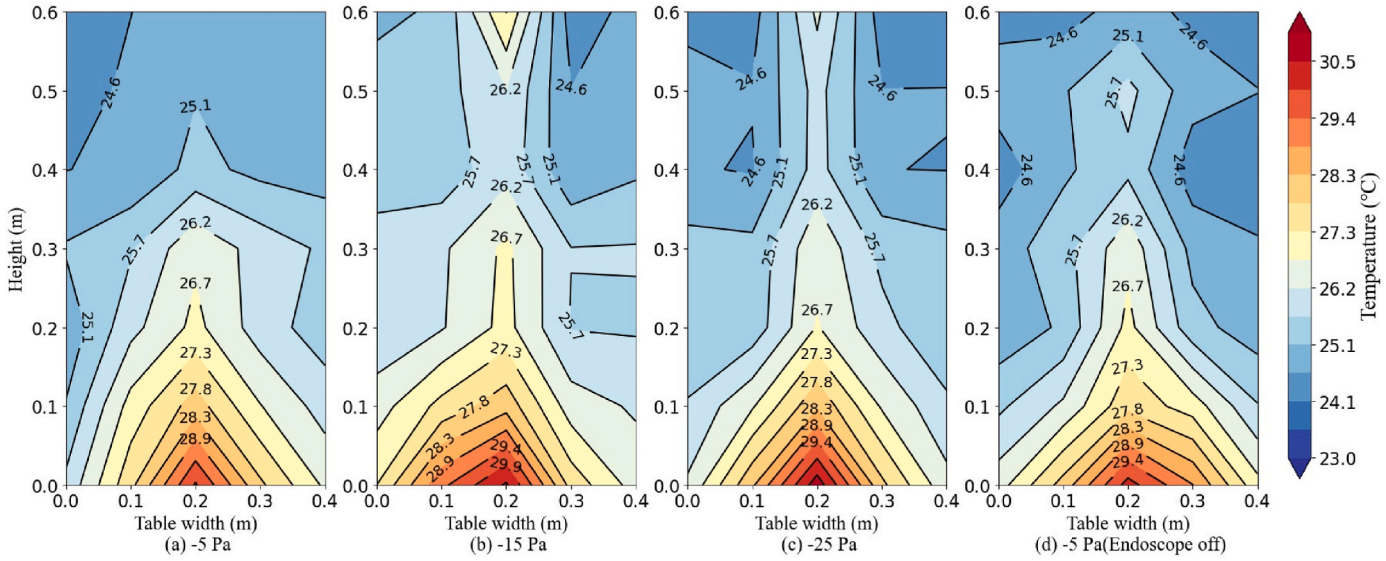

Fig. 7. Contour plot of the temperature distribution of the patient's thermal plume (a) −5 Pa (b) −15 Pa (c) −25 Pa.

found in Appendix 3 and Appendix 4.

3.5. Temperature and velocity distribution of the thermal plume above the wound (Case 4)

Fig. 7 shows the temperature distribution of the thermal plume above the wound. The distribution of the thermal plume presents some similar characteristics under different pressures as well as when the endoscope is turned off. First, the maximum temperature, which was approximately 31 °C, was found at the bottom middle of the measurement area, which was directly above the wound area. Second, as height increases, the temperature decreases, which is a typical feature of the thermal plume. At the initial part of the thermal plume, the temperature gradient is similar. In the height range of 0–0.3 m at three pressure difference conditions, the temperature of the centerline of the thermal plume decreases by approximately 3.7 °C. In addition, the temperature distribution of the thermal plume is symmetric in all cases. However, when the height is greater than 0.3 m, the temperature gradient attenuation varies greatly under different working conditions. At −5 Pa, the temperature is 26.6 °C at 0.3 m and 24.5 °C at 0.6 m, which decreases by 2.1 °C. At a pressure difference of −15 Pa, the centerline temperature of the thermal plume decreases from 26.8 °C (0.3 m) to 26.0 °C (0.4 m) and then increases to 27.3 °C (0.6 m). Similarly, at −25 Pa, the centerline temperature of the thermal plume decreased from 26.6 °C (0.3 m) to 25.8 °C (0.4 m) and then increased to 26.3 °C (0.6 m). When the endoscope was closed, similar characteristics of the patient thermal plume with other cases were observed.

Fig. 8 shows the measured velocity distribution of the thermal plume. Under the three pressure difference conditions, the maximum velocities of the thermal plume are 0.20 m/s, 0.20 m/s, and 0.19 m/s. These maximum values of the velocity of the thermal plume occur at a similar height of 0.4 m but not a similar width. The point with the highest velocity at the −5 Pa condition is at 0.0 m of table width, while under −15 Pa, it occurs at 0.1 m of table width and occurs in the middle of the table width, that is, 0.2 m under −25 Pa. A significant shift toward the center as the differential pressure increases can be seen. In addition, the thermal plume has shifted toward the assistant surgeon at height = 0 m (10 cm above the patient) in the figure. The velocity profile is different from the typical thermal plume velocity distribution, in which the velocity reaches the maximum at the centerline and decreases with increasing height. As the thermal plume deflects toward the assistant surgeon, a slow zone appears in front of the main surgeon's abdomen, where the velocity is less than 0.13 m/s. The airflow velocities in front of the assistant surgeon's nose were 0.18 m/s, 0.18 m/s, and 0.17 m/s under the three working conditions. The airflow velocity in front of the nose of the main surgeon was 0.132 m/s in all three differential pressure situations. The thermal plume velocity distribution was more symmetrical when the endoscope was closed than when the endoscope was turned on at −5 Pa. The maximum velocity of the plume was 0.19 m/s in both cases, but with the endoscope closed it appeared at the highest point along the centerline. In addition, a lower minimum velocity of 0.05 m/s was observed with the endoscope is turned off.

4. Discussion

4.1. Distribution characteristics of tracer gas concentration

From Figs. 3–5, we noticed that many outliers were observed at all test points except the exhaust and distribution nurse breathing zones in all working conditions. In addition, the results of the respiratory zone concentration of the assistant surgeon and the main surgeon showed that the data were skewed, so we could confirm that the data did not follow a normal distribution. Some previous studies measuring air pollutant concentrations have yielded similar results and provided explanations. Air pollutant concentrations are inherently random variables because of their dependence on the fluctuations of a variety of meteorological and emission variables [55]. . It depends on the position, the flow state. The distribution of air pollution is generally a two-parameter lognormal distribution [56]. This phenomenon is very common in contaminant detection, which is explained by the theory of continuous random dilution. According to theory, pollutants are still in the process of being diluted rather than completely mixed [57]. In this study, we observed this phenomenon in the breathing zones of surgical staff near the surgical microenvironment, including an anesthesiologist, assistant surgeon, and main surgeon, which suggests that tracer gas is still in the intermediate stage of dilution when moving to these areas rather than being completely mixed with air. This may indicate that surgical staff who work in proximity to a COVID-19-infected patient may be exposed to a higher coronavirus concentration than those who work further from the patient in ORs with mixing ventilation under negative pressure.

4.2. Influence of pressure difference on exposure level

Table 3 shows the results of the intergroup posttest, indicating whether there was a statistically significant difference between the two groups. Points 1 and 2, regardless of whether the pollutant is released

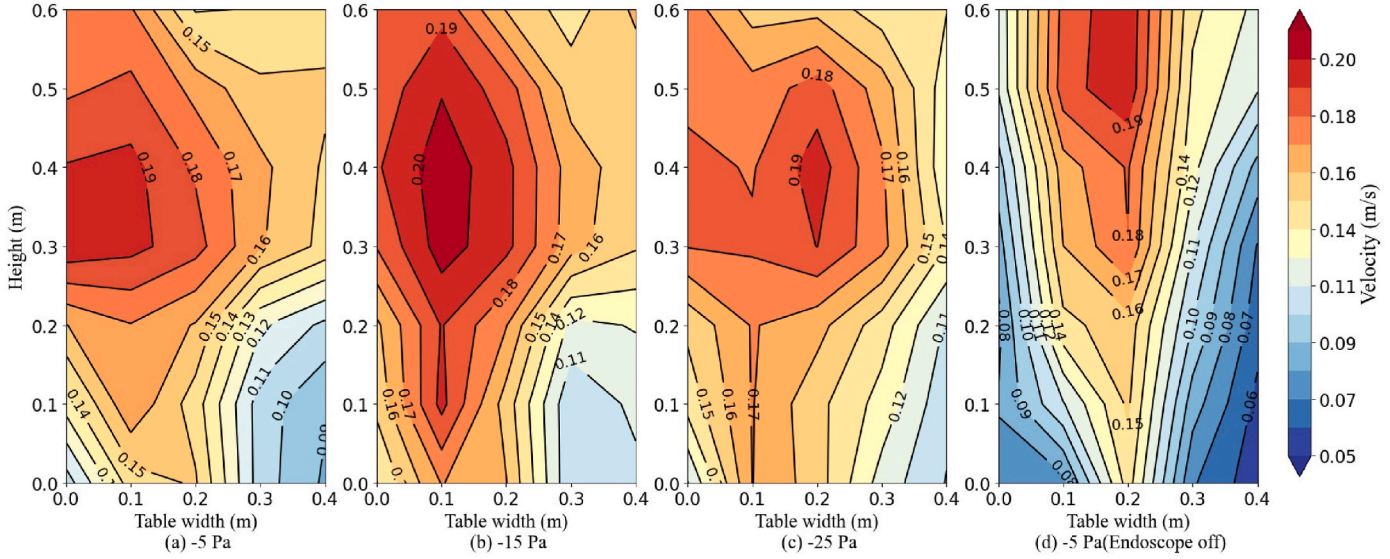

Fig. 8. Contour plot of the velocity distribution of the patient's thermal plume.

Table 3
Data analysis of whether the variation of pressure difference in different positions has a significant effect on the concentration data.

Measurement point	Case #-#					
	1–2	2–3	1–3	4–5	5–6	4–6
1. Exhaust	$p = 0.001$	$p = 0.180$	$p < 0.001$	$p = 0.001$	$p = 0.371$	$p < 0.001$
2. Distribution nurse	$p = 0.003$	$p = 1.000$	$p = 0.006$	$p < 0.001$	$p = 0.823$	$p < 0.001$
3. Anesthesiologist	$p = 0.126$	$p < 0.001$	$p < 0.001$	$p = 0.758$	$p = 0.848$	$p = 0.998$
4. Sterile nurse	$p = 0.807$	$p = 0.098$	$p = 0.127$	$p = 0.538$	$p = 0.001$	$p < 0.001$
5. Main surgeon	$p = 0.039$	$p = 0.008$	$p < 0.001$	$p = 0.301$	$p < 0.001$	$p < 0.001$
6. Assistant surgeon	$p = 0.268$	$p = 0.005$	$p < 0.001$	$P = 0.767$	$p = 0.649$	$p = 0.989$

from the nose or the wound, show similar characteristics. This is easy to understand since both sites are far away from the patient. When the pressure difference changes from −5 Pa to −15 Pa, there is a significant difference between the two groups of data, but when the pressure difference changes from −15 Pa to −25 Pa, there is no significant difference between the two groups of data. According to the actual measured exhaust air volume, we know that there is a small difference in the actual ventilation volume with different pressure differences. The ventilation volume differences between −5 Pa and −15 Pa and between −15 Pa and −25 Pa are 102 m^3/h and 74 m^3/h, respectively. This difference is due to the relationship between the pressure difference and ventilation volume determined by the following equation:

$$\Delta p^{0.5}\delta = Q \tag{1}$$

where Δp is the pressure difference, Pa; Q is the flow rate, m^3/h; and δ is a coefficient. For this experiment, the relationship between the flow rate and pressure difference can be fitted as $63.58\ \Delta p^{0.5} = Q$ ($R = 0.99$). The characteristics of the results at points 1 and 2 may be because the concentration discharge is more sensitive to changes in large ventilation volumes and less sensitive to changes in small ventilation rates.

At point 3, there is a significant difference only between the Case 2 and Case 3 data, while at point 4, there is a significant difference only between the Case 5 and Case 6 data. From the concentration results, such a difference is very small and may be caused by changes in ventilation volume.

On the other hand, according to the results of the local air change index at each point combined with the results of the concentration, with the increase of the pressure difference, the local air change index at point 2 to point 4 increases, and the concentration at each point decreases accordingly. The concentration data can be related to the local air change index. That is, the greater the local air index is, the smaller the concentration. This can explain the influencing factors of indoor concentration at each point, including the actual ventilation volume and air distribution. However, for points 5 and 6, this conclusion does not apply. We did not observe the relationship between the local air change index and concentration data.

When the differential pressure changes from −15 Pa to −25 Pa, the concentration data at point 5 differ significantly regardless of where the tracer gas is released. It can be seen from the thermal plume results that the change of pressure difference can significantly change the characteristics of the patient's thermal plume, which may be due to the influence of airflow infiltration into the gap of the room envelope, and this influence is more intense for point 5 than the change of ventilation rate and the change of the same fraction efficiency. When tracer gas was released from the wound, the concentration data of point 6 did not differ significantly under different pressure differences. This may be due to the Coanda effect on the chest of the assistant surgeon after the thermal plume from the patient's wound is diverted to the assistant surgeon. This effect will not be affected by external airflow.

4.3. Other factors affecting exposure levels

In this study, we observed that pollutant exposure levels of the assistant surgeon were much higher than those of other medical staff, despite the proximity of the assistant surgeon to the main surgeon. Previous studies of smoke from laparoscopic surgery have also pointed to high levels of assistant surgeon exposure to smoke from patients' wounds [58]. Field measurements by et al. at St. Olav Hospital also found that assistant surgeons were significantly more sensitive to particulate matter of various sizes during certain surgeries than other medical staff [59].

A hypothesis was proposed to explain this characteristic based on the concentration comparison results and the thermal plume velocity distribution results under the switching endoscope imager. Due to the operation of the cooling fan of the endoscope imager, the airflow generated by the endoscope imager affects the patient's thermal plume, diverting it to the surgeon at the early stage of development. This deflection directly entrains contaminants from the patient's wound, or the patient's breath, toward the assistant surgeon. The pollutant exposure concentration of the assistant surgeon was much higher than that of other surgical staff.

4.4. Practical limitations

Due to the tracer gas sampling instrument taking samples at intervals of 6 min, it is impossible to capture concentration fluctuations over shorter periods. In addition, the temperature of the indoor wall inevitably increases by 1–2 °C with the ventilation time, and such subtle changes may have different degrees of influence on the results.

In addition, some hypotheses about the influence of the cooling fan on thermal plume formation are proposed based on the experimental results. Moreover, there is much surgical equipment in the operating room, so the airflow distribution will be significantly affected. The formation of the thermal plume in this complex surgical microenvironment needs further research. Research on human thermal plumes in the surgical microenvironment may face several challenges: the influence of ventilation airflow [60], the modeling of thermal plumes [61], human body movement [62], and the effect of environmental temperature [63]. These studies also suggest that the human thermal plume is sensitive to environmental parameters. Therefore, the formation of the thermal plume in a more complex environment needs more in-depth research through computational fluid dynamic (CFD) studies or theoretical studies.

This study only analyzed the distribution tracer gas in the operating room by mixing ventilation with thermal manikins. However, the movement of surgical staff in the operating room is very normal, and it is not clear whether personnel movement will have a great impact on coronavirus distribution in ORs.

The results of this study provide the concentration of tracer gas in the surgical staff breathing zone in the operating room, and the corresponding concentration attenuation can be obtained. Therefore, the infection risk of the surgical staff can be calculated by using an accurate risk assessment model and virus source intensity. Based on the risk of infection, recommendations can be made to the surgical staff on how to choose PPE equipment. However, it is difficult to calculate the precise risk of infection as there is no clear dose-response relationship for inhalation of the SARS-CoV-2. Therefore, risk assessment was not considered in this study.

5. Conclusion

In this paper, the distribution of airborne contamination released by COVID-19 patients in the OR was studied using tracer gas. The contamination sources were the noses and the wound area of the patients, and the concentrations in the breathing zone of surgical staff in the OR were measured. In addition, the velocity distribution and temperature distribution of the patient's thermal plume were measured, and the airflow interference was compared and analyzed. The following conclusion can be drawn.

- Contaminant exposure levels of the sterile nurse and the distribution nurse outside the surgical microenvironment are affected mainly by the ventilation airflow rate. The exposure levels of surgical nurses are sensitive to the ventilation rate. Due to the difference in the local air change index, there are slight differences in the measured concentration of contaminants between each measured nurse, but they are all around the average exhaust concentration.
- The main surgeon, assistant surgeon, and anesthesiologist in the surgical microenvironment had higher exposure levels to the contamination concentrations in their breathing zones, regardless of whether the source was the nose or a wound. The highest exposure concentration may occur for the assistant surgeon, which can be 12 times higher than the exposure level of other surgical staff outside the surgical microenvironment.
- The cooling fan of the endoscope image, which is located nearby, may have a great effect on the exposure level of the assistant surgeon. This may result in asymmetry in the patient's thermal plume, which in turn results in higher concentrations of contaminants in the assistant surgeon's breathing zone than in that of the main surgeon.
- Increasing the differential pressure resulted in lower concentration levels in the breathing zone of the main surgeon and the assistant surgeon. When the contaminant emission source was the nose, the exposure concentration of both the main surgeon and assistant surgeon decreased. When the contaminant emission source is the wound, the concentration level of the assistant surgeon will not be affected by the pressure difference because the thermal plume is biased toward the assistant surgeon.
- It is recommended that patients with COVID-19 should be operated in a negative-pressure ventilated operating room with a large differential pressure during the COVID-19 epidemic to reduce the risk of infection on surgical staff.

CRediT authorship contribution statement

Yang Bi: Investigation, Methodology, Writing – original draft, Conceptualization. **Amar Aganovic:** Formal analysis, Methodology. **Hans Martin Mathisen:** Supervision. **Guangyu Cao:** Conceptualization, Project administration, Supervision, Writing – review & editing.

Declaration of competing interest

The authors declare that they have no known competing financial interests or personal relationships that could have appeared to influence the work reported in this paper.

Acknowledgment

The authors are grateful to the China Scholarship Council for the financial support to Yang Bi (CSC student ID: 202009210006). We greatly appreciate the collaboration with the Operating Room of the Future (FOR) at St. Olavs hospital in Norway.

Appendix A. Supplementary data

Supplementary data to this article can be found online at https://doi.org/10.1016/j.buildenv.2022.109091.

References

[1] Z. Al Maskari, A. Al Blushi, F. Khamis, A. Al Tai, I. Al Salmi, H. Al Harthi, M. Al Saadi, A. Al Mughairy, R. Gutierrez, Z. Al Blushi, Characteristics of healthcare workers infected with COVID-19: a cross-sectional observational study, Int. J. Infect. Dis. 102 (2021) 32–36.

[2] L. Zheng, X. Wang, C. Zhou, Q. Liu, S. Li, Q. Sun, M. Wang, Q. Zhou, W. Wang, Analysis of the infection status of healthcare workers in Wuhan during the COVID-19 outbreak: a cross-sectional study, Clin. Infect. Dis. 71 (16) (2020) 2109–2113.

[3] J. Wong, Q.Y. Goh, Z. Tan, S.A. Lie, Y.C. Tay, S.Y. Ng, C.R. Soh, Preparing for a COVID-19 pandemic: a review of operating room outbreak response measures in a large tertiary hospital in Singapore, Can. J. Anesthesia/J. Can. Anesthésie 67 (6) (2020) 732–745.

[4] R.S. Sikkema, S.D. Pas, D.F. Nieuwenhuijse, Á. O'Toole, J. Verweij, A. van der Linden, I. Chestakova, C. Schapendonk, M. Pronk, P. Lexmond, T. Bestebroer, R. J. Overmars, S. van Nieuwkoop, W. van den Bijllaardt, R.G. Bentvelsen, M.M.L. van Rijen, A.G.M. Buiting, A.J.G. van Oudheusden, B.M. Diederen, A.M.C. Bergmans, A. van der Eijk, R. Molenkamp, A. Rambaut, A. Timen, J.A.J.W. Kluytmans, B. B. Oude Munnink, M.F.Q. Kluytmans van den Bergh, M.P.G. Koopmans, COVID-19 in health-care workers in three hospitals in the south of The Netherlands: a cross-sectional study, Lancet Infect. Dis. 20 (11) (2020) 1273–1280.

[5] H. Cheng, J.W. Clymer, B. Po-Han Chen, B. Sadeghirad, N.C. Ferko, C.G. Cameron, P. Hinoul, Prolonged operative duration is associated with complications: a systematic review and meta-analysis, J. Surg. Res. 229 (2018) 134–144.

[6] L.K. Ti, L.S. Ang, T.W. Foong, B.S.W. Ng, What we do when a COVID-19 patient needs an operation: operating room preparation and guidance, Can. J. Anesthesia/J. Can. Anesthésie 67 (6) (2020) 756–758.

[7] J.D. Forrester, A.K. Nassar, P.M. Maggio, M.T. Hawn, Precautions for operating room team members during the COVID-19 pandemic, J. Am. Coll. Surg. 230 (6) (2020) 1098–1101.

[8] M.E. Awad, J.C.L. Rumley, J.A. Vazquez, J.G. Devine, Perioperative considerations in urgent surgical care of suspected and confirmed COVID-19 orthopaedic patients: operating room protocols and recommendations in the current COVID-19 pandemic, JAAOS - J. Am. Acad. Orthopaed. Surg. 28 (11) (2020).

[9] F.A. Leyva Moraga, E. Leyva Moraga, F. Leyva Moraga, A. Juanz González, J. M. Ibarra Celaya, J.A. Ocejo Gallegos, J.A. Barreras Espinoza, Aerosol box, an operating room security measure in COVID-19 pandemic, World J. Surg. 44 (7) (2020) 2049–2050.

[10] W.S.R.I. Collaborative, Surgery during the COVID-19 pandemic: operating room suggestions from an international Delphi process, Br. J. Surg. 107 (11) (2020) 1450–1458.

[11] T. Greenhalgh, J.L. Jimenez, K.A. Prather, Z. Tufekci, D. Fisman, R. Schooley, Ten scientific reasons in support of airborne transmission of SARS-CoV-2, Lancet 397 (10285) (2021) 1603–1605.

[12] D. Lewis, Is the coronavirus airborne? Experts can't agree, Nature 580 (7802) (2020) 175.

[13] C. Heneghan, E. Spencer, J. Brassey, A. Plüddemann, I. Onakpoya, D. Evans, J. Conly, T. Jefferson, SARS-CoV-2 and the role of airborne transmission: a systematic review [version 1; peer review: 1 approved with reservations, 2 not approved], F1000Research 10 (232) (2021).

[14] J.L. Santarpia, D.N. Rivera, V.L. Herrera, M.J. Morwitzer, H.M. Creager, G. W. Santarpia, K.K. Crown, D.M. Brett-Major, E.R. Schnaubelt, M.J. Broadhurst, J. V. Lawler, S.P. Reid, J.J. Lowe, Aerosol and surface contamination of SARS-CoV-2 observed in quarantine and isolation care, Sci. Rep. 10 (1) (2020), 12732.

[15] Y. Liu, Z. Ning, Y. Chen, M. Guo, Y. Liu, N.K. Gali, L. Sun, Y. Duan, J. Cai, D. Westerdahl, X. Liu, K.-f. Ho, H. Kan, Q. Fu, K. Lan, Aerodynamic Characteristics and RNA Concentration of SARS-CoV-2 Aerosol in Wuhan Hospitals during COVID-19 Outbreak, bioRxiv, 2020, 2020.03.08.982637.

[16] Y. Jiang, H. Wang, Y. Chen, J. He, L. Chen, Y. Liu, X. Hu, A. Li, S. Liu, P. Zhang, H. Zou, S. Hua, Clinical Data on Hospital Environmental Hygiene Monitoring and Medical Staff Protection during the Coronavirus Disease 2019 Outbreak, medRxiv, 2020, 2020.02.25.20028043.

[17] S.L. Miller, W.W. Nazaroff, J.L. Jimenez, A. Boerstra, G. Buonanno, S.J. Dancer, J. Kurnitski, L.C. Marr, L. Morawska, C. Noakes, Transmission of SARS-CoV-2 by inhalation of respiratory aerosol in the Skagit Valley Chorale superspreading event, Indoor Air 31 (2) (2021) 314–323.

[18] Y. Li, H. Qian, J. Hang, X. Chen, P. Cheng, H. Ling, S. Wang, P. Liang, J. Li, S. Xiao, J. Wei, L. Liu, B.J. Cowling, M. Kang, Probable airborne transmission of SARS-CoV-2 in a poorly ventilated restaurant, Build. Environ. 196 (2021), 107788.

[19] P. Azimi, Z. Keshavarz, J.G. Cedeno Laurent, B. Stephens, J.G. Allen, Mechanistic transmission modeling of COVID-19 on the Diamond Princess cruise ship demonstrates the importance of aerosol transmission, Proc. Natl. Acad. Sci. Unit. States Am. 118 (8) (2021), e2015482118.

[20] A.C. Fears, W.B. Klimstra, P. Duprex, A. Hartman, S.C. Weaver, K.C. Plante, D. Mirchandani, J.A. Plante, P.V. Aguilar, D. Fernández, A. Nalca, A. Totura, D. Dyer, B. Kearney, M. Lackemeyer, J.K. Bohannon, R. Johnson, R.F. Garry, D. S. Reed, C.J. Roy, Comparative Dynamic Aerosol Efficiencies of Three Emergent Coronaviruses and the Unusual Persistence of SARS-CoV-2 in Aerosol Suspensions, medRxiv, 2020, 2020.04.13.20063784.

[21] L. Morawska, D.K. Milton, It is time to address airborne transmission of coronavirus disease 2019 (COVID-19), Clin. Infect. Dis. 71 (9) (2020) 2311–2313.

[22] Y. Luo, M. Zhong, [Standardized diagnosis and treatment of colorectal cancer during the outbreak of novel coronavirus pneumonia in Renji hospital], Zhonghua Wei Chang Wai ke Za Zhi = Chin. J. Gastrointestin. Surg. 23 (3) (2020) E003.
[23] Y. Li, J.J. Qin, Z. Wang, Y. Yu, Y.Y. Wen, X.K. Chen, W.X. Liu, Y. Li, [Surgical treatment for esophageal cancer during the outbreak of COVID-19], Zhonghua Zhong liu Za Zhi [Chin. J. Oncol.] 42 (4) (2020) 296–300.
[24] R. Chen, Y. Zhang, L. Huang, B.-h. Cheng, Z.-y. Xia, Q.-t. Meng, Safety and efficacy of different anesthetic regimens for parturients with COVID-19 undergoing Cesarean delivery: a case series of 17 patients, Can. J. Anesthesia/J. Can. Anesthésie 67 (6) (2020) 655–663.
[25] V. Arora, C. Evans, L. Langdale, A. Lee, You need a plan: a stepwise protocol for operating room preparedness during an infectious pandemic, federal practitioner : for the health care professionals of the VA, DoD, and PHS, Perioperat. Care Operat. Room Manag. 37 (5) (2020) 212–218.
[26] S. Al-Benna, Negative pressure rooms and COVID-19, J. Perioperat. Pract. 31 (1–2) (2020) 18–23.
[27] T. Chow, A. Kwan, Z. Lin, W. Bai, Conversion of operating theatre from positive to negative pressure environment, J. Hosp. Infect. 64 (4) (2006) 371–378.
[28] T.-t. Chow, A. Kwan, Z. Lin, W. Bai, A computer evaluation of ventilation performance in a negative-pressure operating theater, Anesth. Analg. 103 (4) (2006) 913–918.
[29] M.o.H.a.U.-R.D.o.t.P.s.R.o. China, Architectural Technical Code for Hospital Clean Operating Department, 2013.
[30] U. National Health Service, Health Technical Memorandum 03-01 Specialised Ventilation for Healthcare Premises Part A: the Concept, Design, Specification, Installation and Acceptance Testing of Healthcare Ventilation Systems, 2021, p. 64.
[31] C.f.D.C.a. Prevention, Guidelines for Preventing the Transmission of Mycobacterium tuberculosis in Health-Care Settings, vol. 2005, 2005, p. 64.
[32] P.H.A.o. Canada, Canadian Tuberculosis Standards 7th Edition, Chapter 15: Prevention and Control of Tuberculosis Transmission in Health Care and Other Settings, p. 23.
[33] R. Barranco, F. Ventura, Covid-19 and infection in health-care workers: an emerging problem, Med. Leg. J. 88 (2) (2020) 65–66.
[34] H.P. Lee, D.Y. Wang, Objective assessment of increase in breathing resistance of N95 respirators on human subjects, Ann. Occup. Hyg. 55 (8) (2011) 917–921.
[35] L.M. Visentin, S.J. Bondy, B. Schwartz, L.J. Morrison, Use of personal protective equipment during infectious disease outbreak and nonoutbreak conditions: a survey of emergency medical technicians, Can. J. Emerg. Med. 11 (1) (2009) 44–56.
[36] N. Castle, R. Owen, M. Hann, S. Clark, D. Reeves, I. Gurney, Impact of chemical, biological, radiation, and nuclear personal protective equipment on the performance of low- and high-dexterity airway and vascular access skills, Resuscitation 80 (11) (2009) 1290–1295.
[37] A.G. Loth, D.B. Guderian, B. Haake, K. Zacharowski, T. Stöver, M. Leinung, Aerosol exposure during surgical tracheotomy in SARS-CoV-2 positive patients, Shock 55 (4) (2021) 472–478.
[38] A. Murr, N.R. Lenze, W.C. Brown, M.W. Gelpi, C.S. Ebert, B.A. Senior, B.D. Thorp, A.M. Zanation, A.J. Kimple, Quantification of aerosol particle concentrations during endoscopic sinonasal surgery in the operating room, Am. J. Rhinol. Allergy 35 (4) (2020) 426–431.
[39] B.C.H. Tsui, S. Pan, Are aerosol-generating procedures safer in an airborne infection isolation room or operating room? Br. J. Anaesth. 125 (6) (2020) e485–e487.
[40] M. Garbey, G. Joerger, S. Furr, A systems approach to assess transport and diffusion of hazardous airborne particles in a large surgical suite: potential impacts on viral airborne transmission, Int. J. Environ. Res. Publ. Health 17 (15) (2020) 5404.
[41] G. Cao, A.M. Nilssen, Z. Cheng, L.-I. Stenstad, A. Radtke, J.G. Skogås, Laminar airflow and mixing ventilation: which is better for operating room airflow distribution near an orthopedic surgical patient? Am. J. Infect. Control 47 (7) (2019) 737–743.
[42] ASHRAE, Standard 55-2020 – Thermal Environmental Conditions for Human Occupancy (ANSI Approved), American Society of Heating, Refrigerating and Air-Conditioning Engineers, 2021.
[43] M. Bivolarova, J. Ondráček, A. Melikov, V. Ždímal, A comparison between tracer gas and aerosol particles distribution indoors: the impact of ventilation rate, interaction of airflows, and presence of objects, Indoor Air 27 (6) (2017) 1201–1212.
[44] C. Noakes, L. Fletcher, P. Sleigh, W. Booth, B. Beato-Arribas, N. Tomlinson, Comparison of tracer techniques for evaluating the behaviour of bioaerosols in hospital isolation rooms, in: Proceedings of Healthy Buildings, Syracuse, 2009, pp. 13–17.
[45] J.W. Tang, C.J. Noakes, P.V. Nielsen, I. Eames, A. Nicolle, Y. Li, G.S. Settles, Observing and quantifying airflows in the infection control of aerosol- and airborne-transmitted diseases: an overview of approaches, J. Hosp. Infect. 77 (3) (2011) 213–222.
[46] A. Aganovic, G. Cao, L.-I. Stenstad, J.G. Skogås, An experimental study on the effects of positioning medical equipment on contaminant exposure of a patient in an operating room with unidirectional downflow, Build. Environ. 165 (2019), 106096.
[47] Y. Zhang, G. Cao, G. Feng, K. Xue, C. Pedersen, H.M. Mathisen, L.-I. Stenstad, J. G. Skogås, The impact of air change rate on the air quality of surgical microenvironment in an operating room with mixing ventilation, J. Build. Eng. 32 (2020), 101770.
[48] R.K. Englehardt, B.M. Nowak, M.V. Seger, F.D. Duperier, Contamination resulting from aerosolized fluid during laparoscopic surgery, J. Soc. Laparoendosc. Surg. 18 (3) (2014) e2014.00361.
[49] ANSI ASHRAE, Standard-170 2017, Ventilation of Healthcare Facilities, ANSI/ASHRAE Atlanta, GA, 2017.
[50] C.f.D. Control, Prevention, Guidelines for Environmental Infection Control in Health-Care Facilities, Centers for Disease Control and Prevention (US), Centers for Disease Control and Prevention (US), 2017.
[51] D.o. Health, Health Technical Memorandum HTM 03-01: Specialised Ventilation for Healthcare Premises, Part A: Design and Validation, 2007.
[52] G, Management Specification of Air Cleaning Technique in Hospitals, 2013.
[53] E. Mundt, H.M. Mathisen, P.V. Nielsen, A. Moser, Ventilation Effectiveness, Rehva, 2004.
[54] A. Novoselac, J. Srebric, Comparison of air exchange efficiency and contaminant removal effectiveness as IAQ indices, Trans.-Am. Soc. Heat. Refrigerat. Air Condit. Eng. 109 (2) (2003) 339–349.
[55] P.G. Georgopoulos, J.H. Seinfeld, Statistical distributions of air pollutant concentrations, Environ. Sci. Technol. 16 (7) (1982) 401A–416A.
[56] W.R. Ott, Environmental Statistics and Data Analysis, Routledge, 2018.
[57] W.R. Ott, A physical explanation of the lognormality of pollutant concentrations, J. Air Waste Manag. Assoc. 40 (10) (1990) 1378–1383.
[58] E.A.F. Van Gestel, E.S. Linssen, M. Creta, K. Poels, L. Godderis, J.J. Weyler, A. De Schryver, J.A.J. Vanoirbeek, Assessment of the absorbed dose after exposure to surgical smoke in an operating room, Toxicol. Lett. 328 (2020) 45–51.
[59] S.F. Ragde, R.B. Jørgensen, S. Føreland, Characterisation of exposure to ultrafine particles from surgical smoke by use of a fast mobility particle sizer, Ann. Occup. Hyg. 60 (7) (2016) 860–874.
[60] J. Ma, H. Qian, P.V. Nielsen, L. Liu, Y. Li, X. Zheng, What dominates personal exposure? Ambient airflow pattern or local human thermal plume, Build. Environ. 196 (2021), 107790.
[61] T.H. Dokka, P.O. Tjelflaat, A simplified model for human induced convective air flows-model PREDICTONS compared to experimental data, in: Proceeding of Room Vent 2002 (8th International Conference on Air Distribution in Rooms), Citeseer, 2002.
[62] Y. Tao, K. Inthavong, J. Tu, A numerical investigation of wind environment around a walking human body, J. Wind Eng. Ind. Aerod. 168 (2017) 9–19.
[63] G. Feng, Y. Bi, Y. Zhang, Y. Cai, K. Huang, Study on the motion law of aerosols produced by human respiration under the action of thermal plume of different intensities, Sustain. Cities Soc. 54 (2020), 101935.